





Numerical Modeling of Face Shield Protection against a Sneeze

Ainara Ugarte-Anero ¹, Unai Fernandez-Gamiz ^{1,*}, Iñigo Aramendia ¹, Ekaitz Zulueta ²
and Jose Manuel Lopez-Guede ²

¹ Nuclear Engineering and Fluid Mechanics Department, University of the Basque Country, UPV/EHU, Nieves Cano 12, Vitoria-Gasteiz, 01006 Araba, Spain; augarte060@ikasle.ehu.eus (A.U.-A.); inigo.aramendia@ehu.eus (I.A.)

² System Engineering and Automation Control Department, University of the Basque Country, UPV/EHU, Nieves Cano 12, Vitoria-Gasteiz, 01006 Araba, Spain; ekaitz.zulueta@ehu.eus (E.Z.); jm.lopez@ehu.eus (J.M.L.-G.)

* Correspondence: unai.fernandez@ehu.eus

Abstract: The protection provided by wearing masks has been a guideline worldwide to prevent the risk of COVID-19 infection. The current work presents an investigation that analyzes the effectiveness of face shields as personal protective equipment. To that end, a multiphase computational fluid dynamic study based on Eulerian–Lagrangian techniques was defined to simulate the spread of the droplets produced by a sneeze. Different scenarios were evaluated where the relative humidity, ambient temperature, evaporation, mass transfer, break up, and turbulent dispersion were taken into account. The saliva that the human body generates was modeled as a saline solution of 8.8 g per 100 mL. In addition, the influence of the wind speed was studied with a soft breeze of 7 km/h and a moderate wind of 14 km/h. The results indicate that the face shield does not provide accurate protection, because only the person who is sneezed on is protected. Moreover, with a wind of 14 km/h, none of the droplets exhaled into the environment hit the face shield, instead, they were deposited onto the neck and face of the wearer. In the presence of an airflow, the droplets exhaled into the environment exceeded the safe distance marked by the WHO. Relative humidity and ambient temperature play an important role in the lifetime of the droplets.

Keywords: COVID-19 protection; face shield; sneeze; droplet evaporation; relative humidity; environment temperature; computational fluid dynamics (CFD)



Citation: Ugarte-Anero, A.; Fernandez-Gamiz, U.; Aramendia, I.; Zulueta, E.; Lopez-Guede, J.M. Numerical Modeling of Face Shield Protection against a Sneeze. *Mathematics* **2021**, *9*, 1582. <https://doi.org/10.3390/math9131582>

Academic Editor: Michael Booty

Received: 6 June 2021

Accepted: 1 July 2021

Published: 5 July 2021

Publisher's Note: MDPI stays neutral with regard to jurisdictional claims in published maps and institutional affiliations.



Copyright: © 2021 by the authors. Licensee MDPI, Basel, Switzerland. This article is an open access article distributed under the terms and conditions of the Creative Commons Attribution (CC BY) license (<https://creativecommons.org/licenses/by/4.0/>).

1. Introduction

Currently, we are experiencing a pandemic caused by the new coronavirus SARS-CoV-2, which causes the disease known as COVID-19. The WHO defines the term pandemic as “the worldwide spread of a new disease”. The expansion and spread of COVID-19 have changed our lifestyle habits. The strategies for combating such a phenomenon are rather limited, and prevention is the best way to control and to reduce the transmission of COVID-19. This is not the first time the world has had to deal with a global situation due to the spread of an infectious disease. During human history there have been several global pandemics such as the Black death, the Spanish flu, and smallpox, among others. According to Saunders-Hastings et al. [1], advances in the medical sector change when it comes to dealing with a pandemic. Verma et al. [2] showed that social distance and hand washing are essential to combat COVID-19, all accompanied by the use of masks. When coughing, sneezing, or even talking, dozens of droplets are exhaled into the environment with a high chance of infecting another human being. These droplets are defined as aerosols, which may be in a liquid or gaseous state. The study of Zhu et al. [3] noted that 6.7 mg of saliva is expelled with each individual sneeze.

The evaporation of these particles causes the reduction of the particle diameter, and this phenomenon depends on the relative humidity and the environmental temperature and flows, according to Wang et al. [4]. Redow et al. [5] observed that when the droplets

leave our mouths their temperature immediately drops, acquiring the temperature of the environment. The study developed by Li et al. [6] showed that once exhaled droplets evaporate and their diameter decreases, there is an increase in the concentration of pathogens per unit volume, leading to an increase in the risk of infection. Wei et al. [7] concluded that in particles below 50 μm , evaporation is most significant. The research carried out by Mowraska et al. [8] claimed that the most important factor to consider in the contagion of a virus is the particle diameter. Xie et al. [9] stressed that the size of a droplet depends on two factors: evaporation and the movement of the droplets. The computational fluid dynamics (CFD) numerical model provided by Chillón et al. [10] indicated that the movement of particles with a diameter of less than 30 μm is governed by the Brownian effect. On the other hand, average particles up to 80 μm are subject to major forces, while larger diameter droplets are affected by gravity. According to Redow et al. [5], droplets with a diameter of 10 μm evaporate at about 550 milliseconds when relative humidity is 80% (very wet environment). They also stated that the same particle, under conditions of 50% relative humidity, evaporates in 300 milliseconds, and in 20% relative humidity in 250 milliseconds. These results are in agreement with the work of Wang et al. [4], assuring that relative humidity is an important factor in evaporation. However, the evaporation of these aerosols does not remove the chance of infection, as shown in the work of Van Doremalen et al. [11]. They determined that SARS-CoV-2 has a half-life of about 1 h in the environment whereas if those aerosols fall on plastic or stainless steel, the half-life will be 6.8 h and 5.6 h, respectively.

Avoiding close contact and maintaining a social distance of 1.83 m (6 feet) are two of the main guidelines to prevent infection. However, Feng et al. [12] observed that larger distances need to be considered due to ventilation conditions or external winds. The results of Li et al. [13] showed that with a wind speed of 2 m/s, a particle of 100 μm could reach up to 6.6 m. The computational model by Dbouk et al. [14] also concluded that with a wind speed between 4 km/h and 15 km/h, the droplets of saliva exhaled into the environment could traverse 6 m. They also noted that particles decrease their concentration in the wind direction. On the other hand, in an enclosed space, that is, when air speed is 0 m/s and when it is not possible to keep the social distance, it is essential to use ventilation strategies to reduce the chance of infection. Sen et al. [15] demonstrated this in their CFD study inside an elevator. When there is a vent, the droplets fall to the ground without impacting any person. In contrast, aerosols would reach the person and could infect them.

However, maintaining a safe social distance without any measure of individual protection is not enough, and, therefore, wearing masks has also been recommended. Principally, there are two types of masks: masks that cover only the mouth, nose, and chin and face shields, which cover the whole face (eyes, nose, and mouth). Regarding the masks that cover the mouth, nose, and chin, there are several types and they offer different functions; for example, surgical masks last 4 h and prevent the exhaled air from being dispersed, whereas the personal protective equipment (PPE) that have three levels of filtering facepiece respirators (FFP1, FFP2, FFP3) vary in their effectiveness at filtration. They filter the inhaled air and protect against the inhalation of aerosols. The face shields, however, are plastic screens with the purpose of covering our faces and acting as a protective barrier against aerosols. Akhtar et al. [16] performed an experimental study to prove the effectiveness of wearing a mask when sneezing. Five different masks were evaluated: surgical, cloth, cloth PM 2.5, wetted cloth PM 2.5, and N95. They showed that the aerosols came out into the environment while wearing all masks except for the N95 mask. The mathematical model by Arumuru et al. [17] agrees with Akhtar et al. [16] in stating that the N95 masks completely prevent leakage of droplets in the direction of advancement, although they observed that the droplets disperse to the environment between the holes of the mask and the nose. The mask recommended by Arumuru et al. [17] that has a lower leakage ratio is the commercial five-layered mask. It can be concluded that when wearing both masks combined, the risk of infection can be reduced. Recently, Salimnia et al. [18] undertook a study on the protection offered by the two types of masks and the protection offered by both combined,

and no improvements were noted when combining them. Arumuru et al. [17] also agrees with Salimnia et al. [18], arguing that the combination of the two masks is not feasible. In contrast, the computational model by Akagi et al. [19] investigated the protection offered by face shields, concluding that this type of mask is not a good protection tool, as 4.4% of the droplets exhaled into the environment enter the gap between the human and the face shield. Wendling et al. [20] carried out an experimental work to compare the barrier performance of face masks and face shields. The experimental data showed that, in a conversation between two people, a mask does not protect the human who sneezes, but the one who is sneezed on is protected. Moreover, when a face shield is used, the protection is better since it reduces the number of particles. Besides, when the human who sneezes is the one who is protected, there is hardly any difference between the two masks.

Several numerical works for multiphase flows coupled with incompressible fluid motion can be found in the literature, such as the convergence analysis of a fully discrete finite difference scheme for the Cahn–Hilliard–Hele–Shaw equation presented by Chen et al. [21] and the error analysis of a mixed finite element method proposed by Feng and Prohl [22]. In that field, Yan et al. [23] showed that a second-order energy-stable scheme for the Cahn–Hilliard–Hele–Shaw equation was able to produce accurate long-time numerical results with a reasonable computational cost. The coupling of the Cahn–Hilliard equation to the Navier–Stokes equation of fluid flow gained the attention of Diegel et al. [24], with a convergence analysis and error estimates for a second-order accurate finite element method.

In the current work, a CFD numerical model is presented with the aim of analyzing the spread of a sneeze containing viral droplets and evaluating the effectiveness of a face shield as a personal protective device. The human who wears the face shield has a height of 1.8 m and is placed at a social distance of 1.5 m from another human. Two scenarios were studied. In the first scenario, the mouths of both individuals are situated at the same height, while in the second scenario the mouths are located at a height difference of 0.2 m. The evaporation of aerosols was checked by modifying the ambient temperature and relative humidity. Two different temperatures were applied, 25 °C and 15 °C, and relative humidity (RH) values of 40% and 60% were studied for each case. In addition, two different wind speeds, 7 km/h and 14 km/h, were added to the numerical model to verify the social distance, with a favorable wind in the same direction as the sneeze.

2. Materials and Methods

2.1. Validation

For the validation of our numerical model, the evaporation of a single droplet over time was numerically simulated. Three different diameters were evaluated: 1 μm , 10 μm , and 100 μm . The temperature of the environment and the droplet were $T_e = 293.15\text{ K}$ and $T_d = 310.15\text{ K}$, respectively. Figure 1 shows the results with four different relative humidity ratios (0%, 20%, 60%, and 80%), the same method used by Redow et al. [5], Mowraska et al. [8], and Li et al. [13].

In addition, the study of Hamey [25] was used to validate the distance that a single droplet can traverse. The study consisted of a free fall water droplet into a wet space of relative humidity $\text{RH} = 70\%$, $T_e = 293\text{ K}$, and $T_d = 289\text{ K}$, and droplet diameter of 110 μm or 115 μm , as shown in Figure 2.

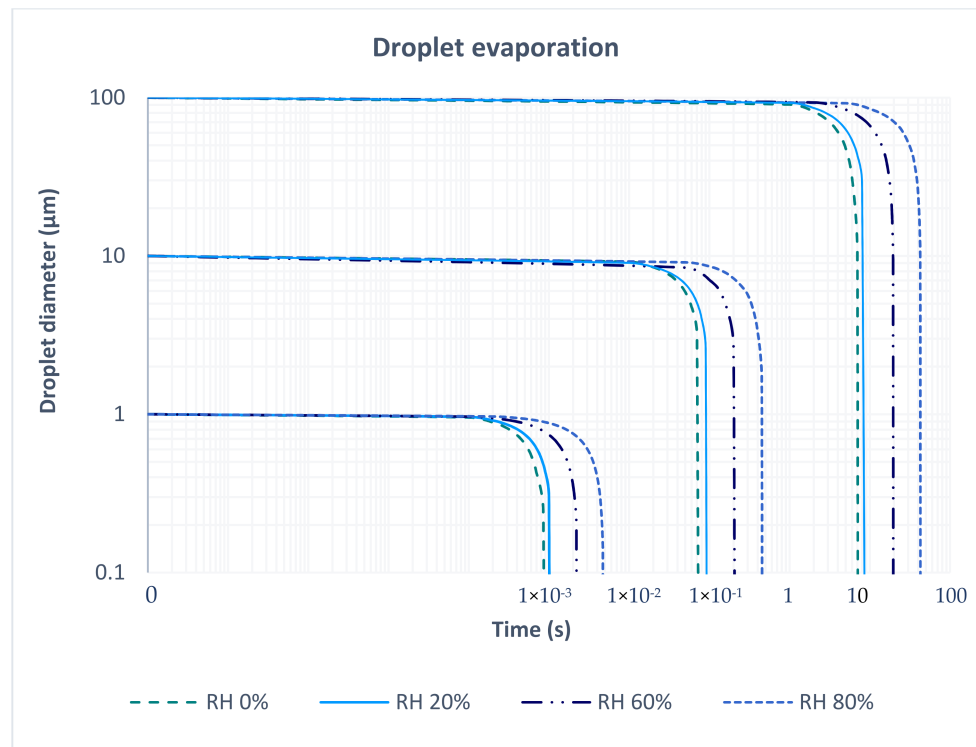


Figure 1. Evaporation of a single pure water droplet under different environment conditions, environment temperature of 293.15 K, particle temperature 310.15 K, and different droplet sizes (1 μm, 10 μm, and 100 μm).

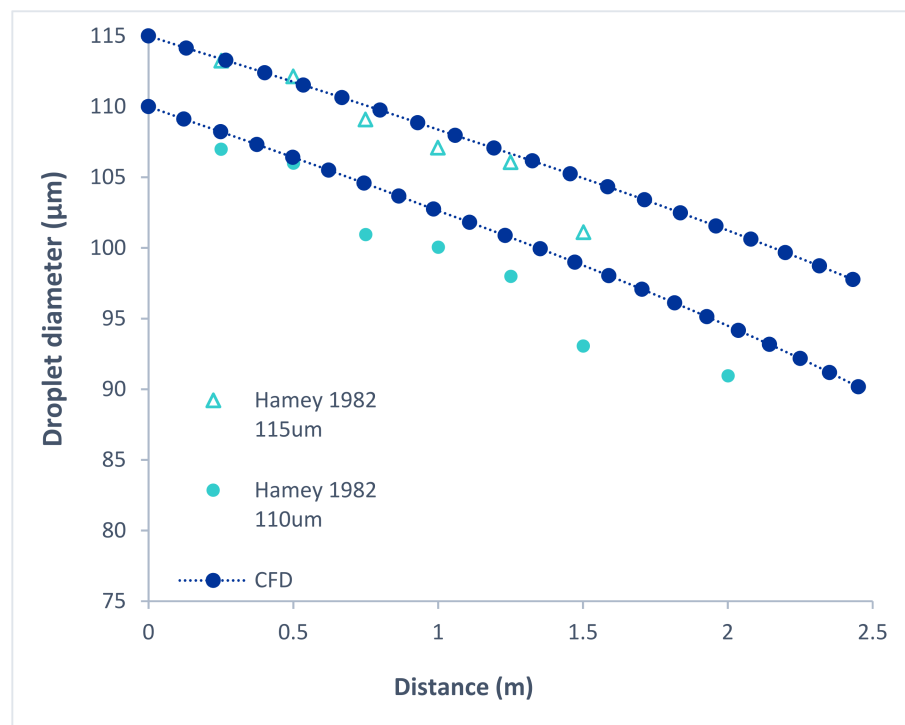


Figure 2. Freely falling water droplets based on the study of Hamey (1982). Particle sizes of 110 μm and 115 μm, environment temperature 293 K, particle temperature 289 K, and 70% relative humidity.

2.2. Computational Domain and Initial Conditions

CFD techniques, based on numerical methods and algorithms, allow for the analysis of complex problems under a wide range of conditions and parameters. In the current work, an individual was placed in an open three-dimensional domain. The domain size was $3\text{ m} \times 2\text{ m} \times 2.5\text{ m}$ (X, Y, Z), but the walls were simulated as a symmetry plane. The human had a height of 1.8 m and the height of its mouth was located at 1.6 m. Figure 3 shows the geometry of the subject and the face shield that it is wearing that covers its whole face. Table 1 shows the main dimensions of the face shield.

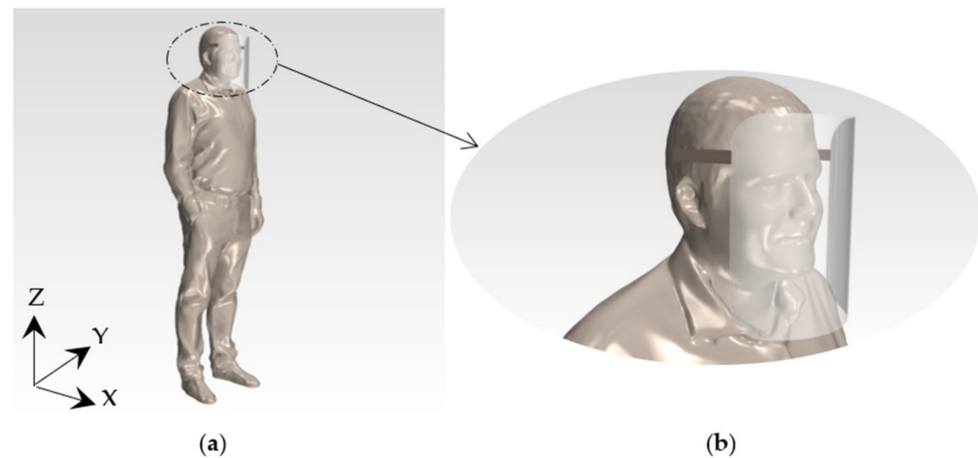


Figure 3. Human geometry: (a) Human body (1.8 m tall); (b) Face shield in detail.

Table 1. Face shield dimensions.

Dimension	Value
Height	250 mm
Length	196 mm
Area	660 mm ²

Another human has been placed in front of the first at a distance of 1.5 m. Only the mouth has been modeled to simulate the sneezing by means of a surface injector, see Figure 4. The aerosols and air jet are exhaled into the environment at a temperature of $36\text{ }^{\circ}\text{C}$, the average temperature of the human body. According to Carpenter et al. [26] saliva is the most characteristic fluid of the body, having to perform the function of taste and being composed of different elements, giving rise to a composition that is difficult to recreate. Nicas et al. [27] summarizes the composition of saliva in water and non-volatile solids. The concentration of ions and cations is 150 mM, which in terms of mass equals 8.8 g/L. In the current study, saliva was modeled as a saline mixture in which it only has influence in reducing the saturation pressure of the water. The mass of each sneeze was 6.7 mg, based on the research of Zhu et al. [3] showing the average mass of aerosols poured into the environment in each sneeze. The mouth geometry was defined as: $DM = 40\text{ mm}$ and $dm = 20\text{ mm}$, as shown in Figure 4c, in order to represent the mouth shape when sneezing. A sneezing velocity condition of 16 m/s with a duration of 400 milliseconds were used. In the first scenario, the mouths of the two individuals were at the same height. With the aim of comparing the effect of the people's height, a second case was modeled with a difference between the height of the two mouths of 20 cm. For each height of mouth, two different temperatures were applied, one warmer at $25\text{ }^{\circ}\text{C}$ and another cooler at $15\text{ }^{\circ}\text{C}$. Since the average suitable relative humidity range is 40–60%, each ambient temperature was simulated first with 40% and then with 60% relative humidity. To model an open space, wind factor was included, giving a comparison between a soft breeze of 7 km/h

and a moderate wind of 14 km/h. The wind had the same direction as the jet exhaled by the subject.

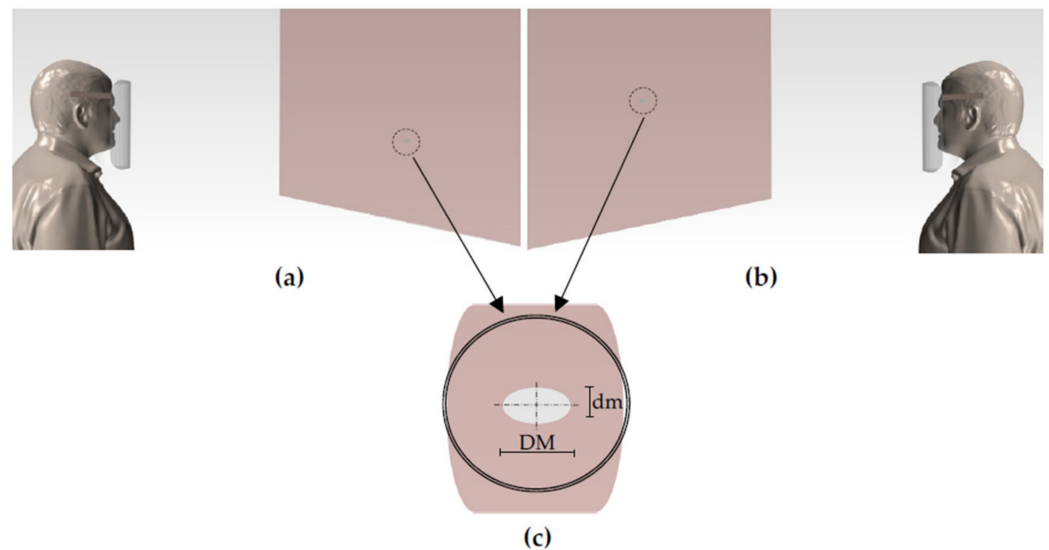


Figure 4. Position of the mouth at 1.5 m: (a) The same height as the human with the face shield, 1.6 m; (b) A difference of height of 20 cm; (c) Geometry of the mouth (DM = 40 mm and dm = 20 mm) to simulate a sneeze.

The discretization of the computational domain was made by means of a trimmer mesh. The domain was composed of 6.7×10^6 (6,755,678) cells. The most important zone of this study was the face shield, where the droplets were expected to impact, therefore, a finer mesh was made near it using a volume control (VC). The same volume control was also used in the direction of sneezing. In addition, a second volume control was used above and below the jet. Figure 5a illustrates the mesh used when the mouths were at the same height and Figure 5b show the meshes used when the difference between the height of the two mouths was 20 cm.

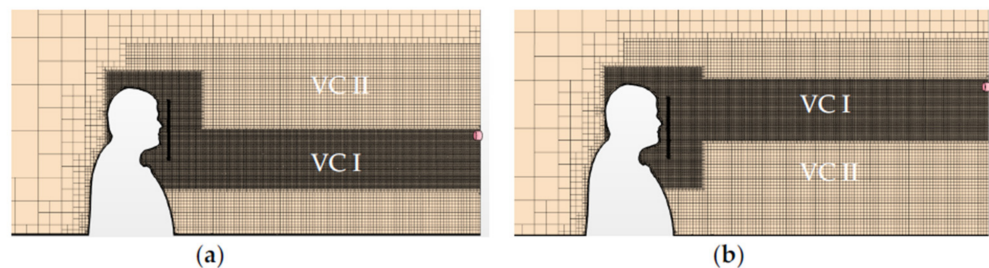


Figure 5. Mesh distribution, the block (■) indicates the mouth of the individual that has the virus and sneezes: (a) The mesh in the domain when the mouths were at the same height; (b) The mesh in the domain when the mouths were at different heights (20 cm difference).

2.3. Numerical Setup

The fundamental laws that govern the mechanics of fluids are the conservation of mass, linear momentum, and energy, see Equations (1)–(3).

$$\frac{\partial \rho}{\partial t} + \nabla \cdot (\rho v) = 0 \tag{1}$$

$$\frac{\partial (\rho v)}{\partial t} + \nabla \cdot (\rho v \otimes v) = \nabla \cdot (pI) + \nabla \cdot T + f_b \tag{2}$$

$$\frac{\partial (\rho E)}{\partial t} + \nabla \cdot (\rho E v) = f_b \cdot v + \nabla \cdot (v \cdot \sigma) - \nabla \cdot q + S_E \tag{3}$$

where ρ is the density, that is, the mass per unit volume, v is the continuum velocity, \otimes denotes the outer product, f_b is the resultant of the body forces per unit volume acting on the continuum, σ is the stress tensor, p is the pressure, T is the viscous stress tensor, E is the total energy per unit mass, q is the heat flux, and S_E is an energy source per unit volume.

The governing equations for the continuous phase, composed of dry air and water vapor, were expressed in Eulerian form, whereas the Lagrangian description was used to solve the dispersed saliva droplets as they crossed the computational domain. This homogeneous composition has, in all cases, the same temperature, pressure, and velocity. This is a non-reacting species; after determining the properties of each species, the properties of the mixture are calculated as a mass function of the mixture's components. To that end, the mass-weighted mixture method proposed by Busco et al. [28] was used, see Equation (4).

$$\Phi_{mix} = \sum_{i=1}^{N=2} \phi_i Y_i. \quad (4)$$

where Y_i is the mass fraction of air and water vapor and ϕ_i is the property values of mixture component. N is the total number of components in the mixture; in this case, $N = 2$.

Relative humidity depends on the initial air and water vapor mass that is present in the environment and the temperature of the airflow. The equilibrium pressure is the most significant parameter that affects it. To calculate the density and viscosity of air, vapor, and liquid water the equations of Kukkonen et al. [29] were used. These properties were updated as the temperature was varied. As was mentioned previously in this section, saliva is composed mainly of water and non-volatile solids. However, in order to simplify the mathematical model, an assumption was made to consider saliva as a saline solution. This factor will only influence the equilibrium pressure of the water since dissolved inorganic salts help to reduce the saturation pressure of the water. Xie et al. [9] showed that the saturation pressure of these droplets can be calculated using Raoult's law.

$$P_{va,s} = X_d P_{va}(T_w) \quad (5)$$

where $P_{va,s}$ is the saturation pressure of the droplet in the saline mixture, P_{va} is the equilibrium pressure of the water at a specific temperature (T_w), and X_d is the mole fraction of the droplet, calculated as shown in Equation (6).

$$X_d = \left(1 + \frac{6im_s M_w}{\pi \rho_L M_s (d_p)^3} \right)^{-1} \quad (6)$$

where M_w and M_s are the molecular weights of water and of solute, respectively; m_s the mass of the solute in the droplet; d_p is the diameter of the particle (droplet), and the ion factor "i" is equal to 2, in this case for the NaCl.

Droplets, which cross the computational domain, were modeled by Lagrangian equations. In order to calculate the interactions between the mixture of dry air and water vapor and the droplets, the two-way coupling model was used. When droplets are exhaled into the environment, evaporation begins due to a temperature difference. Therefore, a quasi-steady evaporation model, which allows droplets to lose mass through evaporation, was introduced and determined by Sherwood's number. Equation (7) expresses the rate of change of droplet mass due to evaporation [28].

$$\dot{m}_p = g^* \times A_s \ln(1 + B) \quad (7)$$

where B is the Spalding transfer number, g^* is the mass transfer conductance, and A_s is the droplet surface area. However, this phenomenon is not the only one that occurs, the droplets may also be distorted and break up under the action of non-uniform surface forces. This behavior was taken into account using the Taylor analogy breakup (TAB) model.

Taylor analogy represents the distortion of a droplet as in a damping spring mass system; it reflects only the basic mode of oscillation of the droplet.

The distance that these droplets can achieve is affected by the dispersion and turbulence they suffer. This effect was introduced in the present work with the addition of the Reynolds-averaged Navier–Stokes (RANS) equations with a k - ω Shear Stress Transport (SST) turbulence model, developed by Menter [30]. The transport equations for the kinetic energy k and the specific dissipation rate ω are shown in Equations (8) and (9).

$$\frac{\partial}{\partial t}(\rho k) + \nabla \cdot (\rho k \bar{v}) = \nabla \cdot [(\mu + \sigma_k \mu_t) \nabla k] + P_k - \rho \beta^* f_{\beta^*} (\omega k - \omega_0 k_0) + S_k \quad (8)$$

$$\frac{\partial}{\partial t}(\rho \omega) + \nabla \cdot (\rho \omega \bar{v}) = \nabla \cdot [(\mu + \sigma_\omega \mu_t) \nabla \omega] + P_\omega - \rho \beta^* f_{\beta^*} (\omega^2 - \omega_0^2) + S_\omega \quad (9)$$

where \bar{v} is the mean velocity, μ is the dynamic viscosity, σ_k , σ_ω , P_k , and P_ω are Production Terms, f_{β^*} is the free-shear modification factor, S_k and S_ω are the user-specified source terms, and k_0 and ω_0 are the ambient turbulence values that counteract turbulence decay.

Considering experimental data shown by Xie et al. [31] and subsequently validated by Dbouk et al. [14], the initial size distribution of the droplets representing the sneezing was modeled using the Rosin–Rammler distribution. Equation (10) shows the expression to define the probability density functions f , also known as the Weibull distribution. A minimum diameter of 10 μm and a maximum diameter of 300 μm were defined.

$$f = \frac{n}{\bar{d}_p} \left(\frac{d_p}{\bar{d}_p} \right)^{n-1} e^{-\left(\frac{d_p}{\bar{d}_p}\right)^n}, \quad n = 8 \quad (10)$$

where \bar{d}_p is the mean diameter and is equal to 80 μm .

The equation of conservation of linear momentum for a material droplet of mass m_p is given by Equation (11).

$$m_p \frac{dv_p}{dt} = F_s + F_b \quad (11)$$

where v_p denotes the instantaneous particle velocity, F_s is the resultant of the forces that act on the surface of the particle, and F_b is the resultant of the body forces.

Spherical particles were assumed and the energy that these spherical particles release is implemented with the correlation of Ranz–Marshall. This correlation is suitable for spherical particles up to $Re \approx 5000$ and was applied in the evolution of the mass of saliva-only droplet particles due to evaporation. This correlation defines the coefficient of heat transfer as a derivative correlation as a function of the Nusselt number. The droplets injected into the computational domain were under the influence of the drag force, defined by Equation (12).

$$F_d = \frac{1}{2} C_d \rho A_p |v_s| v_s \quad (12)$$

where C_d is the drag coefficient of the droplet, ρ is the density of the continuous phase, A_p is the projected area of the droplet, and v_s is the droplet slip velocity ($v_s = v - v_p$) with v being the instantaneous velocity of the continuous phase.

The Schiller–Naumann model was used to calculate this force, the same method employed by Wang et al. [4]. According with Karunarathne et al. [32], this model was used for modelling of the drag between fluid phases in a multiphase flow. Equation (13) shows the expression to calculate the drag coefficient C_d .

$$C_d \begin{cases} \frac{24}{Re}, & Re \leq 1 \\ \frac{24}{Re} (1 + 0.15 Re^{0.687}), & 1 < Re \leq 1000 \\ 0.44, & Re > 1000 \end{cases} \quad (13)$$

where Re is the Reynolds number.

The influence of the gravity force was taken into account as was the turbulent particle dispersion with the exact eddy interaction time. In this work, the commercial CFD code STAR-CCM + v.14.02 (Siemens, London, UK) [33] was used to define and solve the numerical model of aerosols produced by sneezing. A personal server-clustered parallel computer with Intel Xeon © E5-2609 v2 CPU @ 2.5 GHz (16 cores) and 45 GB RAM were used to run all the simulations. Each simulation took about 35 h of computation, with a total time of approximately 24 days.

3. Results

3.1. Effect of Relative Humidity and Environment Temperature in the Droplets' Evaporation

In this section, the influence of relative humidity and ambient temperature are analyzed. To that end, the quantity of particles exhaled and their corresponding diameter were observed. Firstly, a comparison between $t = 0.4$ s, when the sneeze is finished, and $t = 2.5$ s, when most of the droplets have impacted the person, is presented at $T_e = 15$ °C and $RH = 40\%$. Secondly, a comparison is made to evaluate the influence of relative humidity at $t = 2.5$ s in the following scenarios: $T_e = 15$ °C and $RH = 40\%$ and $T_e = 15$ °C and $RH = 60\%$. Finally, a comparison between $T_e = 15$ °C and $RH = 40\%$ and $T_e = 25$ °C and $RH = 40\%$ is presented to see the difference in ambient temperature.

The evolution of the droplets exhaled to the environment was tracked at $t = 0.4$ s and $t = 2.5$ s and are shown in Figure 6, with a droplet size ranging from 19 μm to 96 μm diameter. At $t = 2.5$ s, a maximum droplet size of 92 μm and a minimum droplet size of 19 μm were observed. At $t = 0.4$ s, in contrast, there were no droplets of 19 μm diameter, but 461 droplets of 29 μm were observed. In that timeframe, the evaporation process takes place, and the 29 μm droplets manage to evaporate down to a diameter of 19 μm .

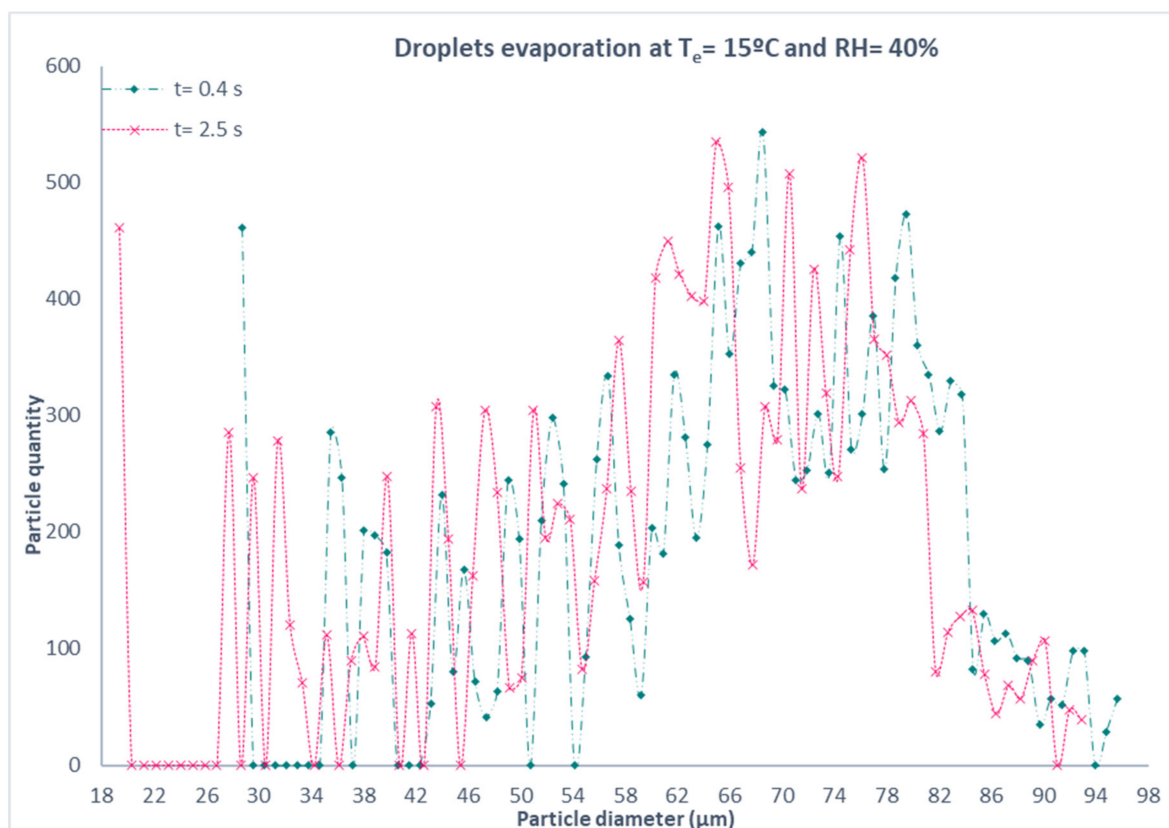


Figure 6. The distribution of the droplets size at $t = 0.4$ s and $t = 2.5$ s when the environment temperature was 15 °C and the relative humidity was 40%.

In Figure 7, the influence of relative humidity can be observed by comparing RH = 40% and RH = 60%. At the same time, with the same ambient temperature conditions and the same sneeze characteristics, droplets of larger diameter were obtained when the relative humidity was higher. Moreover, it can be concluded that an environment with a less relative humidity results in droplets with a smaller diameter. Furthermore, the lifetime of a droplet in the environment at two different temperatures, $T_e = 15\text{ }^\circ\text{C}$ and $T_e = 25\text{ }^\circ\text{C}$, was analyzed as shown in Figure 8. The results determined that droplets with a smaller diameter exist when the temperature in the environment is lower.

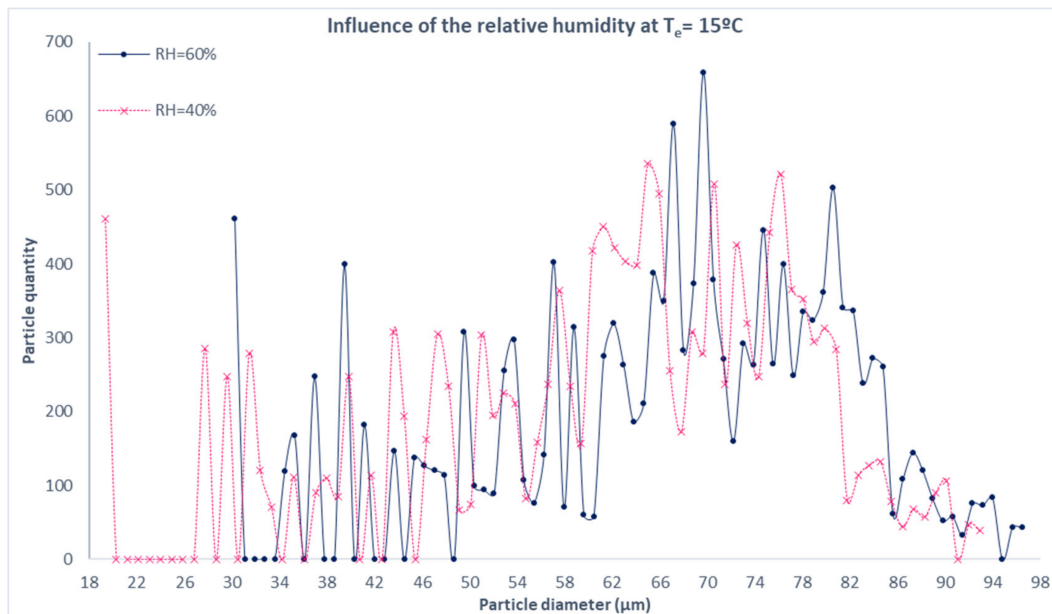


Figure 7. The distribution of the droplets size at $t = 2.5\text{ s}$ when the environment temperature was $15\text{ }^\circ\text{C}$. Comparison between RH = 40% and RH = 60%.

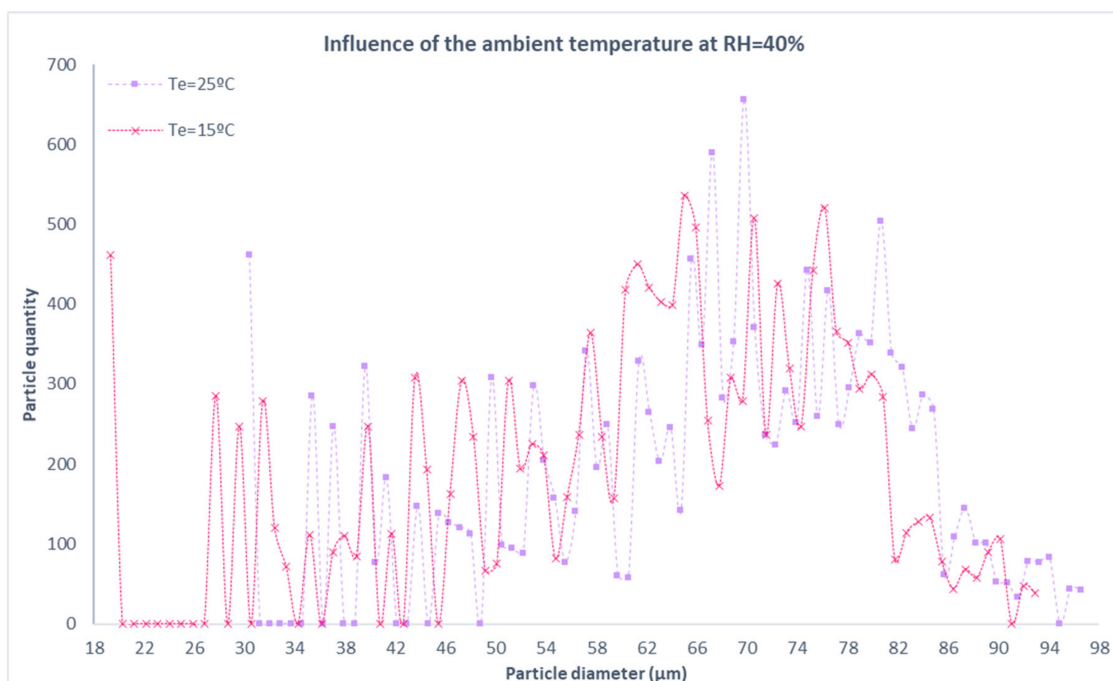


Figure 8. The distribution of the droplets size at $t = 2.5\text{ s}$ when the relative humidity was 40%. Comparison between $T_e = 15\text{ }^\circ\text{C}$ and $T_e = 25\text{ }^\circ\text{C}$.

In addition, in these figures it can be noted that the droplets do not exceed 100 μm in diameter and that, at the end of the sneeze, most of the droplets are present in a size range from 70 μm to 80 μm . Furthermore, in the last second measured in this study, the largest quantity of droplets ranged in size from 60 μm to 70 μm . These results are corroborated with those obtained in the Chillón et al. [10] study, whose data were similar to those obtained in this case. Similar results were also obtained by Xie et al. [9], indicating that droplets in a dry environment take less time to evaporate than in an environment with a high percentage of relative humidity. According to Wang et al. [4], when working with medium-sized droplets, as in the present study, it is quite challenging to precisely know the behavior of these droplets since they are very sensitive to relative humidity.

3.2. Wind Analysis on the Path of the Droplets and a Social Distance Check

The influence of the wind speed in the transmission of the droplets produced with the sneeze was studied with two scenarios: a soft breeze of 7 km/h and a moderate wind of 14 km/h. The sneeze had a velocity value of 16 m/s. When the human sneezes and after 0.4 s, i.e., the time that the sneeze lasts, the droplets immediately adapt to the wind speed; the same result was obtained by Dbouk et al. [14]. In the case of a soft breeze of 7 km/h, droplets traversed the distance of 1.5 m and reached the other human in 0.62 s. When the mouth was placed with a height difference of 20 cm, the droplets arrived earlier, in 0.55 s, as the face shield was closer. With a moderate wind of 14 km/h, the droplets impacted with the silhouette in 0.75 s was due to the turbulence created between the face of the human and the face shield, producing a swirl of droplets that ended up impacting with the back of the face shield. At a different height, the droplets impacted with the face shield in 0.45 s, because the wind speed was considerably higher. Figure 9 illustrates the difference between each wind speed scenario and mouth height. When there is an external airflow, the droplets reach the other human and, therefore, increase the risk of infection. In this study, due to the human placed at a distance of 1.5 m, there is no option to find out how far these droplets can reach. However, our results are in agreement with studies such as those of Feng et al. [12] and Li et al. [13] among others, where the distance of 6 feet is traversed in a very short time.

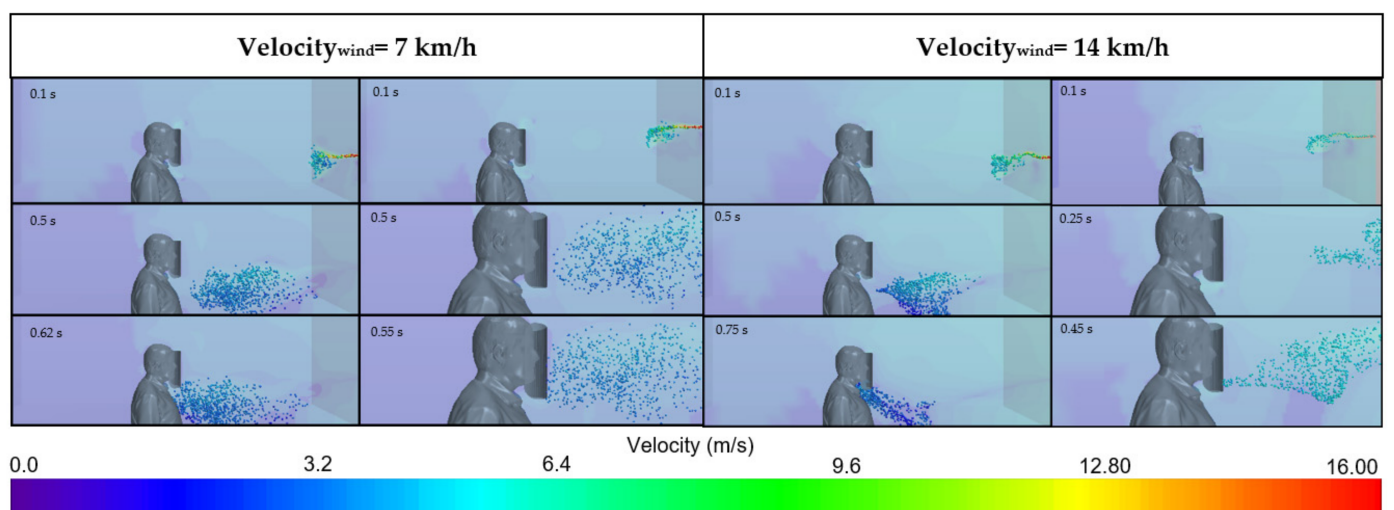


Figure 9. The velocity that the droplets acquire when the relative humidity is 60% and the ambient temperature is 15 °C, at different wind speeds (soft breeze of 7 km/h and moderate wind of 14 km/h). When there was a soft breeze, the droplets reached the other human in 0.62 s and 0.55 s when the human mouths were at the same height and with a height difference of 20 cm, respectively. When there was a moderate wind speed, the droplets reached the other human in 0.75 s and 0.45 s when the human mouths were at the same height and with a height difference of 20 cm, respectively.

3.3. Consequences of People’s Height Difference in Protecting Themselves

The percentage of droplets that impact on the face shield was calculated at $t = 2.5$ s in order to analyze the protection offered by this personal protective equipment. In the case of a soft breeze of 7 km/h and when the mouths of both humans were placed at the same height, the percentage of droplets that hit the face shield was 0.09%. If the mouths were placed at a difference of height of 20 cm, the percentage of droplets that impacted the face shield increased to 10%. Moreover, in a moderate wind scenario of 14 km/h and when the mouths of both humans were located at the same height, there were no droplets impacting inside since all of them entered in the gap between the face of the human and the face shield, depositing on the human neck or on the back of the face shield. When the mouths were located at different heights, the percentage of droplets that impacted with the face shield was 5.5%. Figure 10 shows the area of the face shield occupied by droplets and Figure 11 represents the mass droplets entering the hole and settling on the different parts of the face.

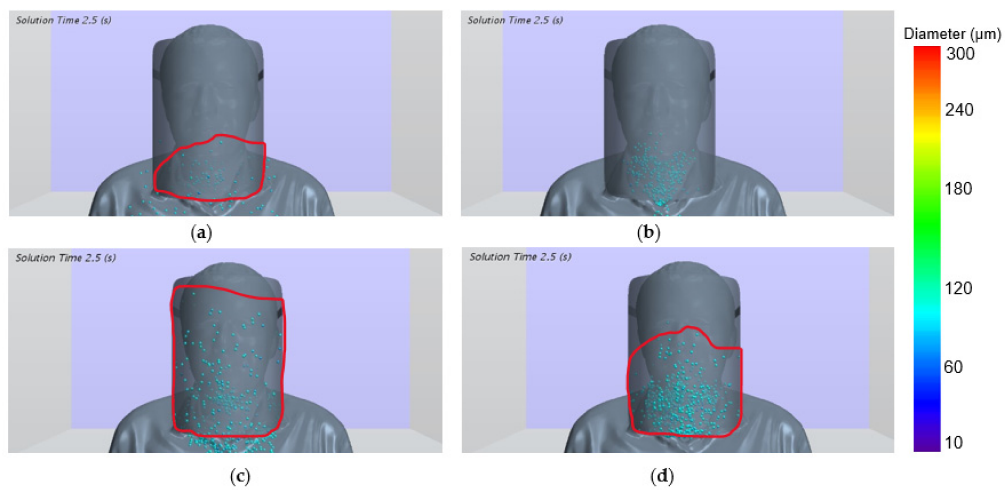


Figure 10. Area of the face shield that protects the human at a 40% RH and $T_e = 25$ °C. (a) Wind speed of 7 km/h and the mouths at the same height; (b) Wind speed of 14 km/h and the mouths at the same height; (c) Wind speed of 7 km/h and the mouths with a height difference of 20 cm; (d) Wind speed of 14 km/h and the mouths with a height difference of 20 cm.

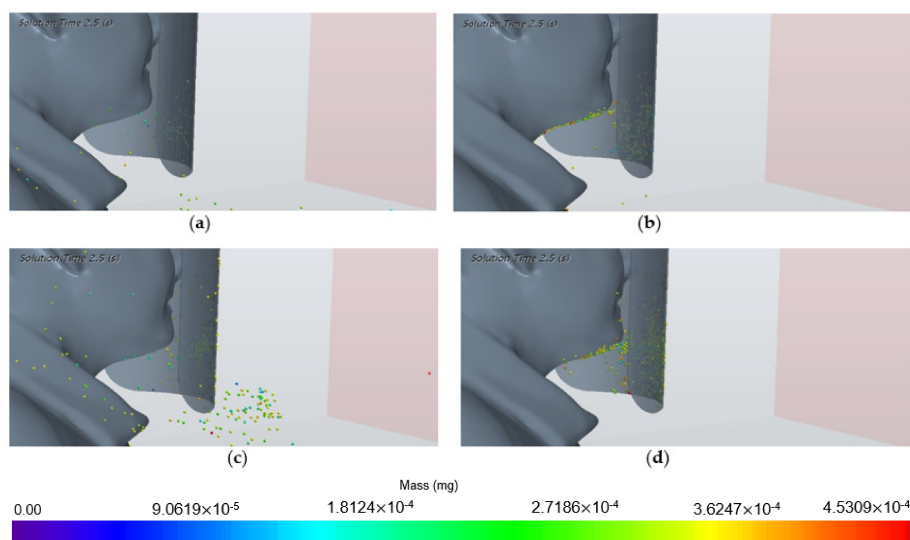


Figure 11. Mass of the droplets entering the face shield at 40% RH and $T_e = 25$ °C. (a) Wind speed of 7 km/h and the mouths at the same height; (b) Wind speed of 14 km/h and the mouths at the same height; (c) Wind speed of 7 km/h and the mouths with a height difference of 20 cm; (d) Wind speed of 14 km/h and the mouths with a height difference of 20 cm.

4. Discussion

Case studies indicate that the spread of SARS-CoV-2 virus via airborne aerosols are a major transmission mechanism for infection [9,12]. According with Ho et al. [34] there is a possible airborne transmission of respiratory droplets where the small airborne droplets ($\leq 5 \mu\text{m}$) stay in the air for a long period of time while droplets larger than $100 \mu\text{m}$ of diameter fall to the ground due to their weight. Small airborne particles and aerosols (diameter $< 5 \mu\text{m}$) can remain for up to several hours in the air, as reported by Jayaweera et al. [35]. Recent studies in the United Kingdom of Great Britain and Northern Ireland reported by the WHO about the B.1.617.2 variant, commonly known as the delta variant, suggest a possible increased risk of severe disease, and support previous observations of increased transmissibility. A recent technical briefing published by the Public Health England [36] shows that the effectiveness against the delta variant is reduced to 31% with the first Pfizer or Astrazeneca vaccine, while with the alpha variant the protection with a single dose is 49%. Once the second dose is supplied, results are improved: 88% protection against symptomatic disease caused by alpha and 80% by delta. Sheikh et al. [37] shows that the risk of transmission increases with respect to the alpha mutation, but mostly affects the young population that has not yet been vaccinated.

The numerical model based on CFD techniques proposed in the current study was defined to evaluate face coverings on airborne transmission risks and, therefore, no empirical or statistical model was included for modeling the rate of infection. Crawford et al. [38] showed that the assessment of the exposure time and/or the minimum viral load required to become infected is relevant. The risk of infection could be found by using a dose-response equation, along with the total amount of virus present in the air and the exposure time; see the case study evaluating the risk of infection by Adhikari et al. [39]. In addition, the infection model in the study of Ho et al. [34] assumes an exponential probability density function for infection as a function of dose, where the infectivity rate is expressed in terms of median infectious dose required to infect 50% of the population.

On the other hand, regarding the different categories of individuals, it must be acknowledged that the current CFD numerical model does not include how the subject inhales the exhaled droplets, and the distribution throughout the respiratory tract depends on the individual. Since the main goal of the study was to evaluate a particular protection system (face shield) when exposed to a sneeze and the aerosol dynamics, no differentiation between gender or age was included.

According to the results obtained in the present work, the droplets exhaled by a sneeze can traverse in barely 1.75 s the safe distance, defined as 1.5 m. The safe distance is a prevention measure that has been updated since the beginning of the pandemic. Currently, and according to the last updated content provided by the WHO on 7 June 2021, maintaining at least a one-meter distance between individuals is recommended to reduce the risk of infection when they cough, sneeze, or speak.

5. Conclusions

In this work, a CFD numerical model based on Eulerian–Lagrangian techniques was presented to analyze the effectiveness of a face shield as personal protective equipment. The Rosin–Rammmler distribution used to define the initial size distribution of the droplets produced by a sneeze of 400 milliseconds showed that all the exhaled droplets are smaller than $100 \mu\text{m}$ in diameter and that those with $70 \mu\text{m}$ are the most representative in terms of particle quantity. In this study, different scenarios were evaluated, varying the relative humidity, 40% and 60%, and varying the ambient temperature, 15°C and 25°C . The numerical model presented in this work showed how at higher relative humidity, the droplets evaporated later. Moreover, at a higher temperature, the droplets' lifetime was higher.

One of the main conclusions obtained with the scenarios studied in this work is that although a social distance of 6 feet is recommended, it is not enough to prevent the contact with viral droplets produced by a sneeze under environmental wind conditions. The numerical model showed how the droplets produced at the end of the sneeze, $t = 0.4 \text{ s}$,

adapt the wind velocity and are able to travel the social distance of 1.5 m between both subjects in less than 1.75 s. The measures to be taken for the prevention of COVID-19 are the use of a mask along with social distance. The conclusions obtained regarding the effectiveness of face shields are that these types of masks do not protect individuals in the case where the transmitter is not protected and the receiver is. Note that in a conversation of two people who are keeping a social distance of 1.5 m and have different personal characteristics such as height, droplets caused by the sneeze of the emitter can enter in the gap between the face of the human and the face shield. Consequently, based on the results obtained in this study, it can be concluded that an individual wearing a face shield is not fully protected and may inhale the viral droplets circulating in the gap between the face of the individual and the face shield.

Author Contributions: Conceptualization, A.U.-A.; methodology, A.U.-A.; software, I.A. and J.M.L.-G.; validation, A.U.-A., I.A. and U.F.-G.; formal analysis, A.U.-A. and I.A.; investigation, A.U.-A. and U.F.-G.; resources, J.M.L.-G. and E.Z.; data curation, E.Z.; writing—original draft preparation, A.U.-A.; writing—review and editing, A.U.-A. and I.A.; visualization, A.U.-A. and E.Z.; supervision, U.F.-G.; project administration, U.F.-G.; funding acquisition, U.F.-G. All authors have read and agreed to the published version of the manuscript.

Funding: The authors were supported by the government of the Basque Country through research grants ELKARTEK 20/71 and ELKARTEK 20/78.

Institutional Review Board Statement: Not applicable.

Informed Consent Statement: Not applicable.

Data Availability Statement: The data presented in this study are available on request from the corresponding author.

Acknowledgments: The authors are grateful for the support provided by SGIker of UPV/EHU.

Conflicts of Interest: The authors declare no conflict of interest.

References

1. Saunders-Hastings, P.R.; Krewski, D. Reviewing the History of Pandemic Influenza: Understanding Patterns of Emergence and Transmission. *Pathogens* **2016**, *5*, 66. [[CrossRef](#)] [[PubMed](#)]
2. Verma, S.; Dhanak, M.; Frankenfield, J. Visualizing droplet dispersal for face shields and masks with exhalation valves. *Phys. Fluids* **2020**, *32*, 91701. [[CrossRef](#)] [[PubMed](#)]
3. Zhu, S.; Kato, S.; Yang, J. Study on transport characteristics of saliva droplets produced by coughing in a calm indoor environment. *Build. Environ.* **2006**, *41*, 1691–1702. [[CrossRef](#)]
4. Wang, B.; Wu, H.; Wan, X. Transport and fate of human expiratory droplets—A modeling approach. *Phys. Fluids* **2020**, *32*, 083307. [[CrossRef](#)]
5. Redrow, J.; Mao, S.; Celik, I.; Posada, J.A.; Feng, Z. Modeling the evaporation and dispersion of airborne sputum droplets expelled from a human cough. *Build. Environ.* **2011**, *46*, 2042–2051. [[CrossRef](#)]
6. Li, X.; Shang, Y.; Yan, Y.; Yang, L.; Tu, J. Modelling of evaporation of cough droplets in inhomogeneous humidity fields using the multi-component Eulerian-Lagrangian approach. *Build. Environ.* **2018**, *128*, 68–76. [[CrossRef](#)]
7. Wei, J.; Li, Y. Enhanced spread of expiratory droplets by turbulence in a cough jet. *Build. Environ.* **2015**, *93*, 86–96. [[CrossRef](#)]
8. Morawska, L. Droplet fate in indoor environments, or can we prevent the spread of infection? *Indoor Air* **2006**, *16*, 335–347. [[CrossRef](#)]
9. Xie, X.; Li, Y.; Chwang, A.T.Y.; Ho, P.L.; Seto, E.H. How far droplets can move in indoor environments—revisiting the Wells evaporation-falling curve. *Indoor Air* **2007**, *17*, 211–225. [[CrossRef](#)]
10. Chillón, S.A.; Ugarte-Anero, A.; Aramendia, I.; Fernandez-Gamiz, U.; Zulueta, E. Numerical Modeling of the Spread of Cough Saliva Droplets in a Calm Confined Space. *Mathematics* **2021**, *9*, 574. [[CrossRef](#)]
11. Van Doremalen, N.; Bushmaker, T.; Morris, D.H.; Holbrook, M.G.; Gamble, A.; Williamson, B.N.; Tamin, A.; Harcourt, J.L.; Thornburg, N.J.; Gerber, S.I. Aerosol and Surface Stability of SARS-CoV-2 as Compared with SARS-CoV-1. *N. Engl. J. Med.* **2020**, *382*, 1564–1567. [[CrossRef](#)]
12. Feng, Y.; Marchal, T.; Sperry, T.; Yi, H. Influence of wind and relative humidity on the social distancing effectiveness to prevent COVID-19 airborne transmission: A numerical study. *J. Aerosol Sci.* **2020**, *147*, 105585. [[CrossRef](#)]
13. Li, H.; Leong, F.Y.; Xu, G.; Ge, Z.; Kang, C.W.; Lim, K.H. Dispersion of evaporating cough droplets in tropical outdoor environment. *Phys. Fluids* **2020**, *32*, 113301. [[CrossRef](#)]
14. Dbouk, T.; Drikakis, D. On coughing and airborne droplet transmission to humans. *Phys. Fluids* **2020**, *32*, 053310. [[CrossRef](#)]

15. Sen, N. Transmission and evaporation of cough droplets in an elevator: Numerical simulations of some possible scenarios. *Phys. Fluids* **2021**, *33*, 033311. [[CrossRef](#)]
16. Akhtar, J.; Garcia, A.L.; Saenz, L.; Kuravi, S.; Shu, F.; Kota, K. Can face masks offer protection from airborne sneeze and cough droplets in close-up, face-to-face human interactions?—A quantitative study. *Phys. Fluids* **2020**, *32*, 127112. [[CrossRef](#)]
17. Arumuru, V.; Pasa, J.; Samantaray, S.S.; Surendrasingh Varma, V. Breathing, virus transmission, and social distancing—An experimental visualization study. *AIP Adv.* **2021**, *11*, 045205. [[CrossRef](#)]
18. Salimnia, H.; Meyer, M.P.; Mitchell, R.; Fairfax, M.R.; Gundel, A.; Guru, N.; Chopra, T. A laboratory model demonstrating the protective effects of surgical masks, face shields, and a combination of both in a speaking simulation. *Am. J. Infect. Control* **2021**, *49*, 409–415. [[CrossRef](#)]
19. Akagi, F.; Haraga, I.; Inage, S.; Akiyoshi, K. Effect of sneezing on the flow around a face shield. *Phys. Fluids* **2020**, *32*, 127105. [[CrossRef](#)]
20. Wendling, J.; Fabacher, T.; Pébay, P.; Cosperec, I.; Rochoy, M. Experimental Efficacy of the Face Shield and the Mask against Emitted and Potentially Received Particles. *Int. J. Environ. Res. Public Health* **2021**, *18*, 1942. [[CrossRef](#)]
21. Chen, W.; Liu, Y.; Wang, C.; Wise, S.M. Convergence analysis of a fully discrete finite difference scheme for the Cahn-Hilliard-Hele-Shaw equation. *Math. Comput.* **2016**, *85*, 2231–2257. [[CrossRef](#)]
22. Feng, X.; Prohl, A. Error analysis of a mixed finite element method for the Cahn-Hilliard equation. *Numer Math* **2004**, *99*, 47–84. [[CrossRef](#)]
23. Yan, Y.; Chen, W.; Wang, C.; Wise, S.M. A Second-Order Energy Stable BDF Numerical Scheme for the Cahn-Hilliard Equation. *Commun. Comput. Phys.* **2018**, *23*. [[CrossRef](#)]
24. Diegel, A.; Wang, C.; Wang, X.; Wise, S. Convergence analysis and error estimates for a second order accurate finite element method for the Cahn-Hilliard-Navier-Stokes system. *Numer. Math.* **2017**, *137*, 495–534. [[CrossRef](#)]
25. Hamey, P.Y. The Evaporation of Airborne Droplets. Master's Thesis, Cranfield Institute of Technology, Bedfordshire, UK, 1982.
26. Carpenter, G.H. The Secretion, Components, and Properties of Saliva. *Annu. Rev. Food Sci. Technol.* **2013**, *4*, 267–276. [[CrossRef](#)] [[PubMed](#)]
27. Nicas, M.; Nazaroff, W.W.; Hubbard, A. Toward Understanding the Risk of Secondary Airborne Infection: Emission of Respirable Pathogens. *J. Occup. Environ. Hyg.* **2005**, *2*, 143–154. [[CrossRef](#)]
28. Busco, G.; Yang, R.; Seo, J.; Hassan, Y.A. Sneezing and asymptomatic virus transmission. *Phys. Fluids* **2020**, *32*, 073309. [[CrossRef](#)] [[PubMed](#)]
29. Kukkonen, J.; Vesala, T.; Kulmala, M. The interdependence of evaporation and settling for airborne freely falling droplets. *J. Aerosol Sci.* **1989**, *20*, 749–763. [[CrossRef](#)]
30. Menter, F.R. Two-equation eddy-viscosity turbulence models for engineering applications. *AIAA J.* **1994**, *32*, 1598–1605. [[CrossRef](#)]
31. Xie, X.; Li, Y.; Sun, H.; Liu, L. Exhaled droplets due to talking and coughing. *J. R. Soc. Interface* **2009**, *6*, S703–S714. [[CrossRef](#)]
32. Karunarathne, S.; Tokheim, L. Comparison of the influence of drag models in CFD simulation of particle mixing and segregation in a rotating cylinder. *Linköping Electron. Conf. Proc.* **2017**, *138*, 151–156. [[CrossRef](#)]
33. Siemens STAR CCM+ Version 14.02. Available online: <http://mdx.plm.automation.siemens.com/> (accessed on 15 March 2021).
34. Ho, C.K. Modeling airborne pathogen transport and transmission risks of SARS-CoV-2. *Appl. Math. Model.* **2021**, *95*, 297–319. [[CrossRef](#)]
35. Jayaweera, M.; Perera, H.; Gunawardana, B.; Manatunge, J. Transmission of COVID-19 virus by droplets and aerosols: A critical review on the unresolved dichotomy. *Environ. Res.* **2020**, *188*, 109819. [[CrossRef](#)]
36. SARS-CoV-2 Variants of Concern and Variants under Investigation in England. *Public Health Engl.* **2021**, *71*.
37. Sheikh, A.; McMennamin, J.; Taylor, B.; Robertson, C. SARS-CoV-2 Delta VOC in Scotland: Demographics, risk of hospital admission, and vaccine effectiveness. *Lancet* **2021**, *397*, 2461–2462. [[CrossRef](#)]
38. Crawford, C.; Vanoli, E.; Decorde, B.; Lancelot, M.; Duprat, C.; Josserand, C.; Jilesen, J.; Bouadma, L.; Timsit, J.O. Modeling of aerosol transmission of airborne pathogens in ICU rooms of COVID-19 patients with acute respiratory failure. *Sci. Rep.* **2021**, *11*, 1–12. [[CrossRef](#)]
39. Adhikari, U.; Chabrelie, A.; Weir, M.; Boehnke, K.; McKenzie, E.; Ikner, L.; Wang, M.; Wang, Q.; Young, K.; Haas, C.N.; et al. A Case Study Evaluating the Risk of Infection from Middle Eastern Respiratory Syndrome Coronavirus (MERS-CoV) in a Hospital Setting through Bioaerosols. *Risk Anal.* **2019**, *39*, 2608–2624. [[CrossRef](#)] [[PubMed](#)]